Modelling ricochet of a cylinder on water using ALE and SPH methods

by

T. DeVuyst, M. Seidl, J.C. Campbell,
L. Papagiannis and R. Vignjevic

reprinted from

THE INTERNATIONAL JOURNAL OF
MULTIPHYSICS

2015: VOLUME 9 NUMBER 3

MULTI-SCIENCE PUBLISHING

Modelling ricochet of a cylinder on water using ALE and SPH methods

T. DeVuyst*, M. Seidl, J.C. Campbell*, L. Papagiannis and R. Vignjevic*
Cranfield University, College Road, MK420AL Cranfield, Bedfordshire, UK
*Brunel University London, Institute of Materials and Manufacturing, Structural Integrity, Granta Park, Great Abington, Cambridge, CB21 6AL, UK
tom.devuyst@brunel.ac.uk

ABSTRACT
The ricochet means the rebound off a surface and is a very important scenario in engineering applications. The specific case of an impact of a solid steel body on a water surface has been chosen for the ricochet example. This solid body hits the water surface with a certain velocity and angle and their dependency on the ricochet behaviour is of interest. This impact scenario can be further developed for more complex impact scenarios, like the ditching of aeroplanes, and has been extensively studied in the past. Due to that fact, it was decided to compare the two numerical analyses with each other; SPH in the internal developed code MCM at Cranfield University with the ALE method in the commercial programme LS-Dyna. The early state of the development was the reason that a 2D model was developed in the 3D solver and therefore verification with another method crucial. Therefore the two simulations were set up and the ricochet behaviour investigated. In contrast to the experimental results, these results demonstrate that independent of the numerical method, both models show an unexpected overproduction of ricochet at higher impact velocities, but agree in their over prediction. The benefits arising out of the collaborative approach of SPH and ALE to describe a problem are presented.

Keywords: Ricochet, Water impact, SPH+FE Method, ALE, Fluid Structure Interaction

1. INTRODUCTION

The phenomenon of the ricochet of projectiles upon impact with a liquid and solid surface has been studied extensively in the past [1] [2]. Its importance lays in the application in different areas, from the water landing of aeroplanes, the so called ditching [18][19][20], to the bouncing of projectiles of trees [1]. Initially the interest in the ricochet and its effects has been focused on military operations. The earliest recordings of ricochet date back to the 16th century showing the application of the phenomenon in military operations; like the famous example of the Wallis Bomb. It happened during WWII that the ricochet of spheres off water was considered by Wallis with the concept of the bouncing ball designed to cause damage to dams; given its complex nature there has also been a general interest in the investigation of the phenomenon. An overview of these initial recordings can be found in [4].

*Corresponding Author: E-mail: m.seidl@cranfield.ac.uk

What all these examples have in common is the high forward velocity upon impact and their low energy loss during impact. Investigations of ricochet of projectiles off water have taken place in the past [5] [6] [4] providing theoretical and experimental results. The interest in ricochet was a result from the availability of experimental data for spheres impact on the water surface [4] [3]. Therefore there is a considerable body of knowledge about the physical behaviour of such a specific geometrical type of impacting body. However, an exact displacement of these spheres could not be captured during these experiments. Numerical results gained from LS-DYNA in the ALE method are compared to existing theories for the phenomenon of ricochet and the experimental results [4][3]. It is shown that the numerical method complements the analytical ricochet prediction of a cylinder [4] [5] [6].

2. RICOCHET

The phenomenon of ricochet appears in many engineering definition of the word ricochet means rebound off a surface. The impact of a solid rigid (non-deformable) body on a liquid surface is investigated in [1]. The liquid surface could be any material in liquid form and is a water surface. The rigid body's rebound is dependent on a high forward velocity and low impact angle [7].

2.1. SCENARIO 1: RICOCHET

The solid body hits the water surface with an impact angle θ. After impact the solid body ricochets with and exit angle is $\theta_{ex} \simeq 0.9°$ [3]. Hereby the body can either touch the water surface or sink in before it exits it (Figure 1 a). Moreover after rebound of the water surface the rigid body could still sink in the water due to gravity (Figure 1 b). As it exits the water in the first place, it is seen as a ricochet case [6].

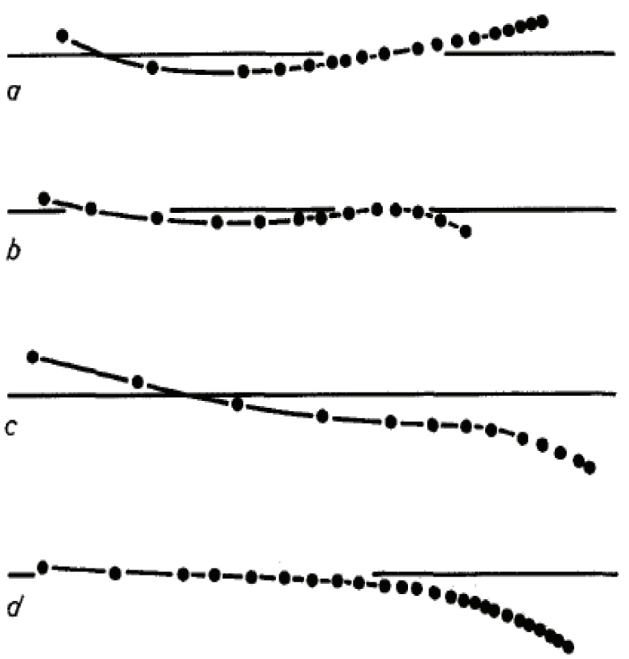

Figure 1: Trajectory possibilities upon impact of cylinder or sphere on water [8]

2.2. SCENARIO 2: SINK OR NON-RICOCHET

There are two different cases showing how the body sinks in the water [6]. One describes that the rigid body slides along the water surface (Figure 1 d). Although it does not sink straight away it is a non-ricochet case. The other describes the immediate sinking of the impacting body, with a slight change of its trajectory (Figure 1 c).

Several studies investigating the phenomena of ricochet have been carried out on the explicit example of impact on the water surface. The first approach of a prediction of a limit of when a body would ricochet from a liquid surface was proposed by Birkhoff et al. [6]. His approach takes in account the density of the impacting body and target. Applied in this scenario, the densities are steel for the sphere ρ_{st} and water ρ_{H_2O}. Applying the two physical density values in the Eqn 1 an overall limit occurs, which is the critical angle $\theta_c = 7.8°$. The body sinks regardless of the impact velocity upon that critical angle θ_c.

$$\theta_c = 17.5 \cdot \sqrt{\frac{\rho_{H_2O}}{\rho_{st}}} \tag{1}$$

This analytical model was extended by the sphere's weight and the impact velocity by Soliman et al. [3]; assuming no angular velocity (no spin) Eqn 2 is obtained. Next the derivation of a theoretical estimate for the critical angle of a non-spinning cylinder and its influence on the velocity will be described. Hutchings [5] developed a theoretical estimate for a spinning cylinder based on the work of Rayleigh [8] [9]; however, the coupling of the angular and linear velocities does not allow for the derivation of the critical angle of a non-spinning cylinder by just neglecting the angular component.

$$\theta_c^2 = \frac{\rho_{H_2O}}{\rho_{st}} - \frac{4 \cdot r \cdot g}{\overline{v}^2} \tag{2}$$

The derivation from L. Papagiannis [10] is given by a pressure p averaged value in the denominator as proposed by Hutchings [5].

This is shown in Eqn 3 taking in account the gravity g, the radius of the cylinder r and its mean velocity $\overline{v}$.

$$\theta_c^2 = \frac{4 \cdot \rho_{H_2O}}{\rho_{st}} \left(\frac{1}{15} - \frac{1}{25} \right) - \frac{2 \cdot r \cdot g}{\overline{v}^2} \tag{3}$$

These theoretical estimates have been applied to the case of projectile having the density of steel (Table 1). For a cylinder without spin, the critical angle is θc = 6.3°. As already mentioned, the dependency on the ricochet scenario of the impact angle and the initial velocity is basis of interest. The graph visualizes the analytical scenarios (Figure 2). First the estimation of Birkhoff (1) states the boundary of the ricochet case of a steel sphere on a water surface, only taking the initial impact angle into account [4][8]. Then the analytical approach for the 3D case (2), the impact of a steel sphere on water is plotted, which takes the impact angle and the initial velocity into account [5]. The analytical models were compared with experimental data [3].

The visualization of the experimental data and the analytical models show an agreement in the critical angle θ_c, that the steel body will not ricochet regardless of its initial velocity with an impact angle of $\theta > 7°$. Also for a $\theta < 2°$ an agreement on the dependency of the initial

Table 1: Model definition of ALE and SPH for the fluid representation

	ALE	SPH
	0.5 mm element size	0.5 mm particle spacing
Water	800 m × 100 mm × 1 mm	800 m × 100 mm × 1 mm
	320000 elements	320000 particles
	Eulerian fixed mesh(AMMG)	Lagrangian formulation
	2nd AMMG	–
Vacuum	800 m × 50 mm × 1 mm	–
	160000 elements	–
Boundary	constrained nodes	symmetry planes
Interaction with cylinder	coupling	contact

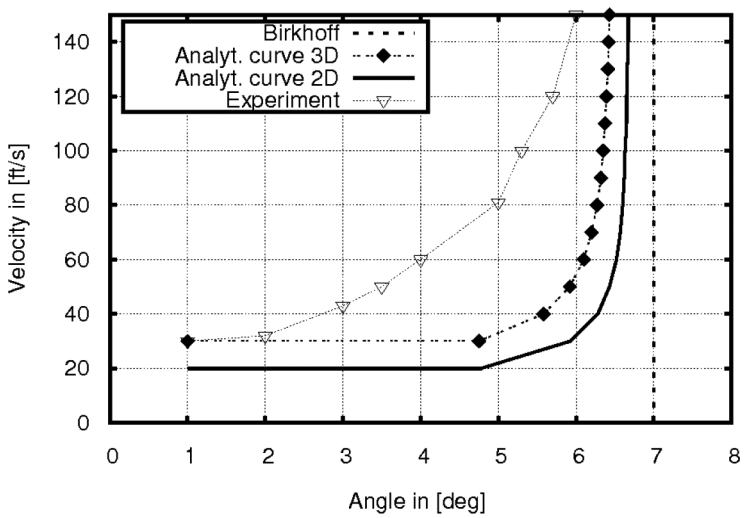

Figure 2: Analytical models plotted with experimental data for 2D and 3D impact case on water

velocity, if the body enters the water with a velocity $v = 30\frac{ft}{s} = 9.1\frac{m}{s}$, ricochet is expected. The ricochet case was of especial interest because of following reasons: First, the high forward velocity of body requires a large fluid domain and that means a challenging example in computational costs. Second, the ricochet has similarities to other fluid structure impact cases e.g. ditching of aeroplanes and the model can therefore be further developed for other applications. Third, the well-defined initial conditions (size and material of rigid body, physical values of fluid) make it an interesting setting, as the important parameters for the simulation are the densities of the materials, the impact angle and speed and finally experimental data is available [3].

Therefore it was chosen to compare the ALE (Arbitrary Lagrangian Eulerian) and SPH (Smooth Particle Hydrodynamics) methods. The SPH code was developed in Cranfield, called MCM (Meshless Continuum Mechanics) and compared to the ALE method in LS-DYNA. That provides the possibility to discuss the results independently of the numerical method. Given the good results LS-Dyna has produced in the past and its ALE capability

[11], it was used for computing impact of a solid Lagrangian body and its ricochet behaviour of the water surface.

3. SPH FORMULATIONS

The convolution principle or interpolant integral are the basis where the SPH method is built upon. The smoothed value $<\psi>(x,t)$ in Eqn 4 gives an estimation on the exact physical field $\Psi(x, t)$ depending on the three- dimensional position vector x and the time t. [12].

$$<\psi>(x,t) = \int \psi(s) \cdot W(x-s,h)\, ds \tag{4}$$

$W(x - s, h)$ is the kernel distribution, with W the so called smoothing kernel function. The support of the kernel is $D_h W$. The value h is the smoothing length, which defines the size of the kernel support.

The smoothing kernel function W is an even function and satisfies first the normalization condition (Eqn 4) and the integration produce the unity in Eqn 5.

$$\int W(x-s,h)\, ds = 1 \tag{5}$$

When the smoothing length h approaches zero, the smoothing kernel function W fulfils a delta function condition in Eqn 6.

$$\lim W(x-s,h)\, ds = \delta(x-s) \tag{6}$$

In order that the smoothing function is a non-zero function a constant C is introduced and this area for integration is called support domain (Eqn 6). On other words, the integration over the problem domain is localised as integration over the support domain of the smoothing kernel function W.

$$W(x-s,h)\, ds = 0 \quad when \quad |x-s| > C \cdot h \tag{7}$$

The kernel is symmetric and several formulations for the equation of motion exist [12]. The conservation laws for conventional SPH are for mass (Eqn 8), momentum (Eqn 9) and energy (Eqn 10).

$$\frac{d\rho_i}{dt_j} = \rho_i \frac{\sum m_j}{\rho_j}\left(v_j - v_i\right)\frac{\partial W_{ij}}{\partial \mathrm{x}} \tag{8}$$

W_{ij} is the kernel smoothing function of particle i evaluated at particle j. For the momentum equation (Eqn 9) the Greek superscripts α and β are introduced to state the coordinate directions.

$$\frac{d\rho_i^{\alpha}}{dt_j} = \sum m_j \left(\frac{\sigma_j^{\alpha\beta} - q_j}{\rho_j^2} + \frac{\alpha_i^{\alpha\beta} - q_i}{\rho_i^2} \right) \frac{\partial W_{ij}}{\partial x^{\beta}} \tag{9}$$

With $\sigma^{\alpha\beta}$ being the total stress tensor:

$$\frac{dE_i^{\alpha}}{dt} = \frac{\sigma_i^{\alpha\beta}}{\rho_i^2} \sum m_j \left(v_j^{\alpha} - v_i^{\beta}\right) \frac{\partial W_{ij}}{\partial x^{\beta}} \tag{10}$$

A Murnghan quasi incompressible equation of state is used (Eqn 11), and this equation is used to calculate the initial condition of the fluid, specifically the spherical component of stress, the pressure p in $\sigma^{\alpha\beta}$. The fluid domain is defined with the physical properties of water and assumed is a non-viscous flow.

$$p = B\left(\frac{\rho}{\rho_o}\right)^{\gamma} - 1 \tag{11}$$

The adiabatic coefficient γ was set to the value of 4 and B is the bulk modulus. Smoothing length of the particles was set to 1.5.

4. NUMERICAL SIMULATIONS

4.1. FLUID DOMAIN

The SPH fluid domain was transformed from the FE (Finite Element) model form that problem, so started with the FE approach, more precisely the ALE (Arbitrary Lagrangian Eulerian) method. The ALE capability gives different design approaches to simulate impact on water [7]. Here, two rectangular parts were defined with solid, cubic, 8 node elements of 0.5 mm length are used for the Eulerian grid [11]. The first part is the water with a size of 800 m × 100 mm × 1 mm, where the cylinder impacts and this part will be transferred to create SPH particles. The other one is vacuum, to let the fluid distribute outside its initial domain. The Eulerian grid contains 480000 cubic solid elements and the SPH with 320000 particles (Table 1).

Vacuum and water (Table 2) are set as AMMG (ALE multi material groups) for each material; allowing the water entering the vacuum region and vice versa. Contact nodes between water and the vacuum are merged, to allow the fluids to travel in the Eulerian grid between the parts. The SPH model consists of one Lagrangian fluid part and the particle motion is calculated in a Lagrangian description. Boundary conditions are set with constrained nodes in ALE and symmetry-planes in SPH. The basin in ALE has fully constrained nodes at its free surfaces and the vacuum unconstrained, letting the fluid exit the fixed Eulerian mesh. The exception is the section surface in xy-plane, where the nodes of water and vacuum are constrained in z translation. For the SPH simulation, five symmetry planes constrain the basin and the surface where the cylinder impacts can distribute the particles in x and y translation. Before the actual transient simulation the water was loaded with gravity to obtain the correct initial conditions, using a dynamic relaxation for both numerical models.

4.2. LAGRANGIAN BODY

In these simulations the mass of the 2D non-spinning projectile was calculated for a solid, rigid cylinder with a length equal to the particle spacing, in effect considering a slice of an infinitely long cylinder. The Lagrangian body has the same position and physical properties for ALE and SPH approach. It has 80 cubic elements on its circumference and a radius of 24.5 mm. Two element rows in z-direction are defined to provide a better performance for coupling [9] in ALE and contact in SPH [12]. The Lagrangian body is constrained globally in the z-direction having two translational degree of freedom in x and y direction [13].

The initial loading of the rigid cylinder are a velocity, split in a horizontal and vertical component, defining the impact angle as such and a gravity force F_g with a constant value over time. Additionally in the ALE mesh, the cylinder is 0.1 mm on both sides in z-direction

Table 2: Material model definitions for water and steel

Material	Parameter	Value	Units
Water	Density	10^{-6}	$\frac{kg}{mm^3}$
	Bulk modulus	$5.5 \cdot 10^{-5}$	$\frac{kN}{mm^2}$
Steel	Density	$5.6 \cdot 10^{-6}$	$\frac{kg}{mm^3}$
	Young's modulus	210	$\frac{kN}{mm^2}$
	Poisson ratio	0.33	

larger than the Eulerian mesh to avoid leakage. Therefore the cylinder which is used in the simulation has a 0.7 mm thickness instead the required 0.5 mm and its mass is adjusted with a value or density:

$$\rho_{0.7\,\mathrm{mm}} = \frac{5}{7} \cdot \rho_{0.5\,\mathrm{mm}} = 5.57 \cdot 10^{-6}\ \frac{kg}{mm^3}$$

and its properties are kept constant for the SPH approach (Table 2).

The contact between fluid and Lagrangian body is a penalty based coupling method (Eqn 12) [14] which is recommended [13] with a coupling direction in compression only [11]. A penalty force F (Eqn 12) is represented by the spring stiffness k [15] and the penetration x, which is similar to the penalty contact.

$$F = k \cdot x \tag{12}$$

The Lagrangian body has the same position and physical properties in ALE as in SPH. The contact between fluid and cylinder is, unlike coupling in ALE (Eqn 12), performed with a contact algorithm. In [16] it is shown the FE-nodes can be treated as SPH particles to effectively model contact between FE and SPH materials.

$$\frac{dv_i}{dt} = \left[\sum m_j \left(\frac{\sigma_j}{\rho_j} + \frac{\sigma_i}{\rho_i} \right) \nabla W_{ij} \right] - \frac{f_{ci}}{m_i} \tag{13}$$

Contact algorithm for SPH code (Eqn 13) works by penalising the momentum equation (1st term of right hand side (RHS)) by a repulsive contact force (2nd term of RHS) [17]. The parameter f_{ci} is a repulsive force.

5. RESULTS

The simulation results were processed to determine whether the particular cylinder impact conditions results sinking or non-ricochet and ricochet. Ricochet and non-ricochet cases were distinguished accordingly to the trajectory of the Lagrangian body. Here, two scenarios were picked, chosen a value of $\theta = 5°$. This angle is an interesting scenario, as there is a disagreement between the analytical and experimental prediction as pointed out earlier (see

Figure 2). At that specific angle, two initial velocities were chosen, $v = 20\frac{ft}{s} = 6.1\frac{m}{s}$ for the non-ricochet case $v = 30\frac{ft}{s} = 9.1\frac{m}{s}$ for the ricochet.

5.1. SINK OR NON-RICOCHET

First shown is the initial position of the Lagrangian body at first touch with the water surface (Figure 3).

At t = 100 ms the sink case could be distinguished and the case is plotted with both numerical methods (Figure 4).

There are some differences in the performance of the simulation, where SPH shows a higher tendency to distribute the particles more freely, whereas the fluid in ALE seems smoother. However, considering that here are two different numerical methods shown, the trajectory of the Lagrangian body were comparable.

5.2. RICOCHET

Also the ricochet scenario, which occurs for the same impact angle θ = 5° with an initial velocity $v = 30\frac{ft}{s}$, is shown in Figure 5. The rebound of the water surface can be distinguished earlier, at t = 60 ms.

Figure 3: Maximum pressure of cylinder on water with a) ALE and b) SPH at θ = 5° and $v = 20\frac{ft}{s} = 6.1\frac{m}{s}$; at t = 15 ms

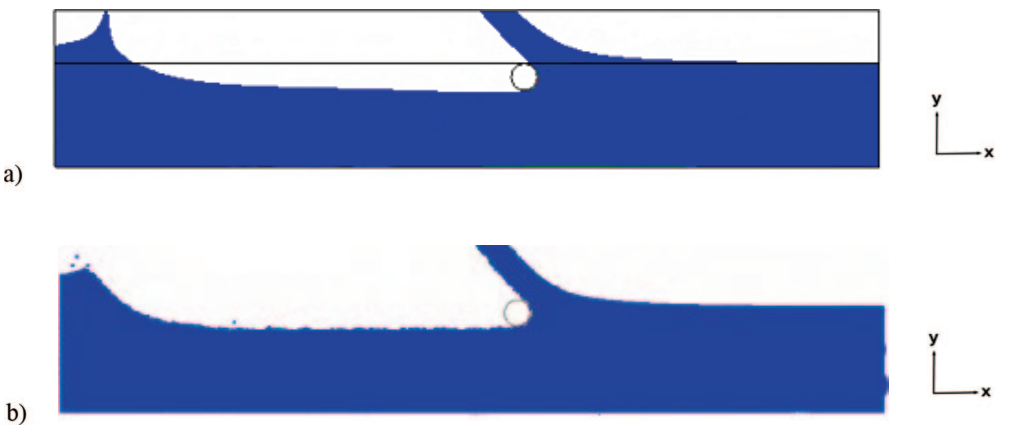

Figure 4: Maximum pressure of cylinder on water with a) ALE and b) SPH at θ =5° and velocity $v = 20\frac{ft}{s} = 6.1\frac{m}{s}$ at t ≈ 100 ms, where the sink case was distinguishable

5.3. COMPARISON

Other impact scenarios with impact angles from 2 to 9 degrees and impact velocities of 15 to 60 feet per second were analysed in the same way to determine whether they resulted in, either sinking or ricochet. These results are shown in graphical format in Figure 6 and 7 where the boundary between sinking and ricochet is marked with a dotted line. The dotted curve was repeated from the SPH result (Figure 7) and plotted again in ALE (Figure 6). It is seen, that prediction of ricochet, circles, and sink, triangles, is similar for both numerical methods. Additionally the analytical boundary was plotted in the graph (Figure 6 and Figure 7) and both methods show an over-prediction of the ricochet behaviour for higher impact velocities.

Figure 5: Maximum impact pressure of cylinder on water with a) ALE and b) SPH at θ =5° and velocity $v = 30\frac{ft}{s}$ at t ≈ 60 ms

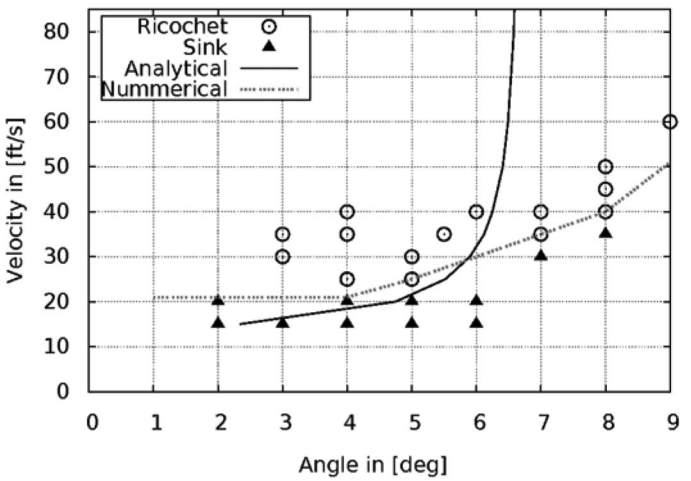

Figure 6: ALE ricochet perdition of cylinder; triangles for sink and circles for ricochet; dotted line shows ricochet behaviour compared to analytical curve

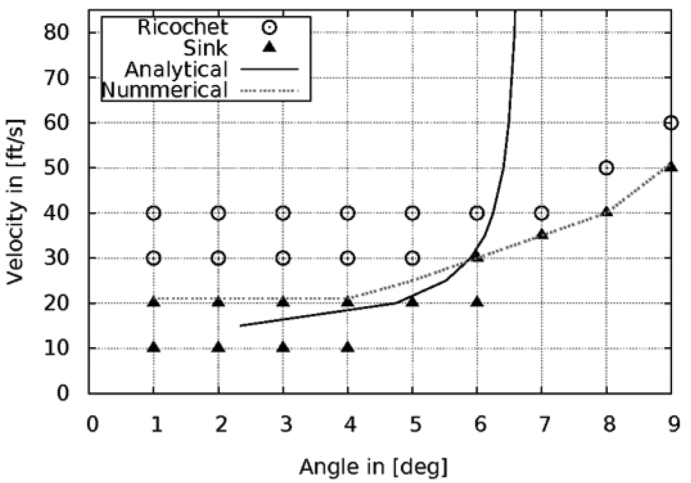

Figure 7: SPH ricochet perdition of cylinder; triangles for sink and circles for ricochet; dotted line shows ricochet behaviour of ALE model

For impact angle of $\theta = 1°$ to $\theta = 4°$ the behaviour shows for the numerical results that the boundary between ricochet and non-ricochet case is a parallel to the abscissa. That fits with the analytical model, were the square root reaches a negative value and the boundary line becomes a parallel line.

The prediction of the analytical model suggests a value of $v = 15 \frac{ft}{s}$ were the numerical model in SPH and ALE show the boundary at $v = 25 \frac{ft}{s}$. From $\theta = 5°$ the incline of the boundary is much steeper in the analytical approach, showing a full sinking behavioural for angles $\theta > 7°$. That fits the prediction of Birkhoff. The incline of the numerical model is

flatter and suggests that there is no direct boundary as such. Due to easier computational accesses the ALE model was extended and showed for the 2D the boundary of $\theta > 13°$. Hence, that regardless of the initial velocity, the cylinder will show ricochet. The boundary of the 2D model contradicts the analytical boundary in the ALE model. These could have different causes; one might be that the assumed contact area in the analytical models, which was initially taken from an investigation for plain surfaces [8], which might not be the right approach for the contact surfaces in 2D. However, both numerical approaches showed the same behaviour.

6. DISCUSSION AND CONCLUSION

Ricochet is a challenging and interesting topic in numerical simulations. The high forward velocity of the impacting body requires a large fluid domain. Moreover, the ricochet of solid bodies on water is a topic, which can be applied for further interesting problems in engineering, like the ditching of aeroplanes. Therefore, to predict reliably the behaviour of solid bodies which ricochet on water surfaces, has been intensively studied in the past.

Here, analytical models were taken and compared for the 2D case with two numerical approaches, one in an Eulerian FE-model and the other in a meshless SPH model. The SPH code was development at Cranfield University. Both numerical models showed a prediction of ricochet behaviour for higher impact angles in the 2D model when compared to an analytical model.

The paper demonstrates successfully, that the numerical ricochet model in SPH could be verified with a numerical model using the ALE method since the two very different mathematical approaches showed a comparable behaviour of ricochet for the 2D case.

Although there are differences in the performance, e.g. the trajectory, both numerical methods agreed in their prediction of ricochet to our satisfaction.

REFERNECES

[1] Gold R. E., Schecter M. D., and Schecter B., Ricochet dynamics for the nine-millimetre parabellum bullet. Journal of Forensic Sciences, JFSCA, 1992, 37(1):90–98.

[2] Bruke T. W. and Rowe W., Bullet ricochet: A comprehensive review. Journal of Forensic Sciences, JFSCA, 1992, 37(5):1254–1261.

[3] Soliman A. S., Reid S. R. and Johnshon W., The effect of spherical projectile speed in ricochet off water and sand. Int. J. Mechanical Science, 18(1):279, 1976.

[4] Johnshon W. and Reid S.R., Ricochet of Spheres off Water, Journal of Mechanical Engineering Science, 1975, 17(2):71–81.

[5] Hutching I. M., The ricochet of spheres and cylinders from the surface of water. Int. J. mech. ScL, 1976, 18:243–247.

[6] Johnshon W., The ricochet of spinning and non-spinning spherical projectiles, mainly from water (part ii). Int. J. Impact Engng, 1998, 21(1–2):25–34.

[7] Do I. and Day J., Overview of ALE method in LS-DYNA – ALE and Fluid-Stucture Interaction Modelling, Livermore Software Technology Corporation (LSTC), 2005.

[8] Lord Rayleigh. On the resistance of fluids. Philosophical Magazine, 1876. 2(13):430–441.

[9] Lord Rayleigh. On the instability of cylindrical fluid surfaces. Philosophical Magazine, 1892, 34 (207):177–180.

[10] L. Papagiannis. *Predicting Aircraft Structural Response to Water Impact*, PhD thesis, Cranfield University, 2014.

[11] Reid J.D. LS-DYNA Examples Manual. Livermore Software Technology Corporation (LSTC), March 1998.

[12] Vuyst T. D. and Vignjevic R., On interpolation in SPH, 2001, CMES, 2(3):319–336.

[13] Gladman B., LS-DYNA Keyword User's Manual, Volume 1. Livermore Software Technology Corporation (LSTC), Livermore, California, 2007.

[14] Souli M. Longatte L. and Verreman V. Time marching for simulation of fluid-structure interaction problems. Journal of Fluids and Structures, 2009, 25(1):95–111.

[15] Benson D.J., Computational Methods in lagrangian and eulerian hydrocodes. Computer Methods in Applied Mech. and Eng., 1992, 99:235–394.

[16] Vuyst T. D., Vignjevic R. and Campbell J., Coupling between meshless and finite element methods. Int. J. of Impact Engng, 2005, 31:1054–1064.

[17] Vuyst T. D., *Hydrocode Modelling of Water Impact*, PhD thesis, Cranfield University, 2003.

[18] K. Hughes, R. Vignjevic, J. C. Campbell, T. De Vuyst, N. Djordjevic, and L. Papagiannis. Bridging the numerical simulation gaps - simulation advancements for fluid structure interaction problems. *International Journal of Impact Engineering*, 2013, 61:48-63.

[19] J.C. Campbell and R. Vignjevic. Simulating structural response to water impact. *International Journal of Impact Engineering*, 2012, 49:1-10.

[20] J.C. Campbell, R. Vignjevic, M. Patel, and S. Milsavljevic. Simulation of water loading on deformable structures using sph. *Computer Modeling In Engineering and Sciences*, 2009, 49:1-21.